

Semi-batch test of sedimentation. Application to design

R. Font*, M.L. Laveda

Department of Chemical Engineering, University of Alicante, Apartado Correos 99, 03080 Alicante, Spain

Abstract

In a batch test of sedimentation with flocculated suspensions, from the evolution of the supernatant-suspension discontinuity height with time, it is possible to obtain the design parameters for continuous gravity thickeners. Nevertheless, the design is only approximate because normally the surface height of the sediment, growing on the bottom of the cylinder, is not visible. On the other hand, the design corresponds to sediment heights much smaller than the initial height of the batch tests, and consequently to very small sediment heights. In the method presented in this paper, the semi-batch test is carried out with periodical withdrawals of supernatant and additions of fresh suspension at the top of the liquid, obtaining a zig-zag variation. Considering the Kynch theorems, that are applicable to the suspension above the sediment, it is possible to obtain the variation of the sediment surface height versus time, and this sediment height can be close to the initial height of the suspension. In this way, it is possible to obtain the exact relationship between the settling flux density of solids in the hindered settling or non-compression zone, and consequently the design parameters for a continuous thickener can be obtained for an underflow solids concentration range and sediment height range wider than those obtained from a batch test. © 2000 Elsevier Science B.V. All rights reserved.

Keywords: Sedimentation; Semi-batch test; Thickener; Design

1. Introduction

This paper discusses a procedure of design of continuous gravity thickeners for opaque suspensions from a semi-batch test.

For the design of continuous gravity thickeners, two main parameters have been considered: the calculation of the cross area and the sediment height.

Considering the cross area, the following procedures can be considered:

- from a batch test or several batch tests of sedimentation considering the upper discontinuity height-time variation: Talmage and Fitch [1], Fitch [2], Merta and Ziolo [3,4].
- from a batch test or several batch tests, taking also into account the sediment height-time curve: Fitch [5], Font [6], Yong et al. [7].
- from the settling flux density-solids concentration curve, that must be obtained previously: Coe and Clavenger [8], Donald et al. [9], Dixon [10], Waters and Galvin [11].

With respect to the calculation of the sediment height inside the continuous gravity thickeners, the following procedures can be distinguished:

- from the data of a batch test, considering only the upper discontinuity variation of the sediment in a batch test: Foust et al. [12], Merta and Ziolo [3].

- from the data of the sediment height in a batch test: Font [13].
- from the effective solids pressure-solids concentration and permeability-solids concentration relationships or similar ones obtained previously: Fitch [14], Landman et al [15], Tiller and Chen [16].

On the other hand, some interesting aspects have been considered for the design of continuous thickeners: effect of sludge funneling [17], dynamic analysis [18], free-settling regime [19], simulation [20,21].

In this section a brief revision of the fundamentals of sedimentation is presented [2,6,13,22–26]. Two ranges of solids concentration are considered in the sedimentation of flocculated suspensions:

(a) at low and intermediate solids concentration, the aggregates descend separately but hinder themselves. For each suspension, there is a relationship between the settling rate and the solids concentration. The inertial effects of acceleration or deceleration can be considered negligible for many suspensions. This range of solids concentration is known as the hindered settling range, or non-compression range.

(b) at high solids concentration, the solids descend forming a matrix of solids. The sedimentation velocity depends on the solids concentration as well as on the pressure transmitted by the weight of the solids of the upper layers and the drag force caused by the fluid moving upwards. This range is called the compression range.

* Corresponding author. Tel.: +34-96-5903546; fax: +34-96-5903464.
E-mail address: rafael.font@ua.es (R. Font).

Nomenclature

A	cross area of cylinder, m
A_u	unit area of continuous thickener, m ² cross area/(m ³ solids/s)
g	gravity acceleration, m/s ²
H	height of descending interface, m
H_i	intercept height of tangent to curve $H_2=f(t_2)$ on time axis
H_0	initial value of H , m
H_u	height of the compression zone in the gravity thickener, m
H_1, H_2	values of H at t_1 and t_2 , m
H_2^*	intercept height between the tangent to sediment at the bottom and the upper interface, m
H_{12}	intercept height between parallel line to height axis that passes through (t_1, L_1) and tangent to curve $H_2=f(t_2)$ in a batch test, m
j	parameter in Eq. (11)
j_0	parameter in Eq. (11)
k	permeability, m ²
L	sediment height, m
L_1	sediment height at time t_1 , m
p_B	parameter in Eq. (12)
p_s	effective pressure of solids, N/m ²
t	time, s
t_1, t_2	values of t at intersection of characteristic with sediment (t_1) and upper interface (t_2), s
t^+	dimensionless time
u_s	settling velocity of solids, m/s
u_{s0}	settling velocity of solids at dilution infinity, m/s
u_{s2}	value of u_s at upper interface; $u_{s2}=dH_2/dt_2$, m/s
S	settling flux density ($=(-u_s)\phi_s$), m/s
x	distance to the bottom, m
x^+	dimensionless distance to the bottom
ΔV	increment of fresh added volume, m ³
<i>Greek letters</i>	
ε_s	volume fraction of solids in the compression range
ε_{s1}	value of ε_s at sediment surface
ε_{su}	underflow volume fraction of solids
$\varepsilon_{s\infty}$	maximum value of volume fraction of solids, defined by Eq. (12)
v	arising velocity of the characteristic line at t_1 , m/s
ϕ_s	volume fraction of solids in the non-compression range
ϕ_{s0}	initial volume fraction of solids
ϕ_{s2}	value of ϕ_s corresponding to characteristic lines that arise from sediment
ϕ_{s2}^*	value of ϕ_s corresponding to characteristic line that arises from bottom of column tangentially to sediment
μ	viscosity of fluid, kg/m s
θ	thickener volumetric flux density of solids, (m ³ solids/s)/m ²
$\Delta\rho$	difference between the solids density and the fluid density, kg/m ³

Symbols

$()^*$	referring to the characteristic that arises tangentially to the sediment surface from the bottom of the cylinder.
$()^+$	referring to the dimensionless variables using the space coordinate and time defined by Eqs. (14) and (17).

The limit of solids concentration between the hindered settling zone and the compression zone is the critical or gel solids concentration, and corresponds to that when the aggregates are in the suspension as a fixed bed and begin to transmit squeeze to the lower layers of solids.

In batch testing, where the initial suspension has a solids concentration in the non-compression range, the sediment

builds up inside the cylinder whereas the upper interface supernatant–suspension descends (see Figs. 1 and 2).

In non-opaque suspensions, the interface corresponding to the sediment surface is visible. Using irradiation equipment or extracting samples at different heights of the cylinder, it is also possible to determine the situation of the sediment surface. In tests where there is a considerable change of sed-

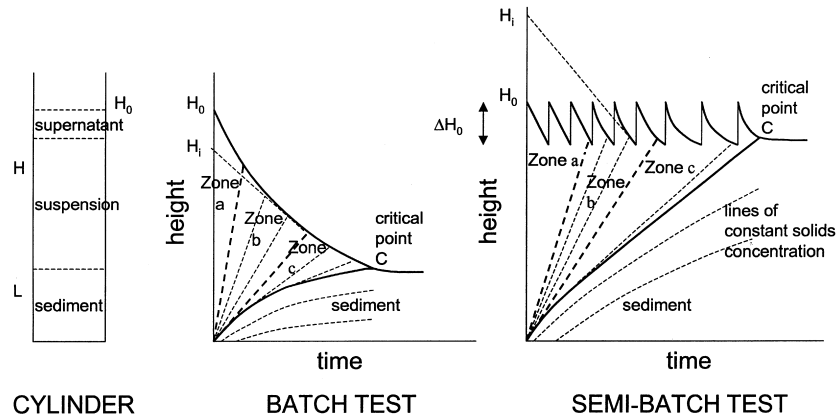


Fig. 1. Batch test and semi-batch test. Symbols used in zones a and b.

imentation velocity of the solids at the upper discontinuity at the critical point (see point C in Fig. 1), the evolution of the sediment surface can be deduced from some batch tests with different initial heights as proposed by Fitch [5].

In previous papers [6,25], a method was proposed for calculating the area per unit of solids volumetric flow and the sediment height of a continuous thickener from data of a batch test (supernatant–suspension discontinuity height vs. time and sediment height vs. time). In a subsequent paper [27], a method using a semi-batch test of sedimentation was proposed for the design of continuous gravity thickeners. The semi-batch test was carried out with periodical withdrawals of supernatant and additions of fresh suspension at the top of the liquid, obtaining a zigzag variation of the supernatant–suspension interface and a convex sediment curve. Initially the cylinder contained a uniform suspension with volume fraction of solids ϕ_{s0} less than the critical or gel concentration ε_{s1} ; then periodically a small volume ΔV of the supernatant was withdrawn (e.g. with a small tube located on the upper supernatant–suspension interface and connected to a vacuum pump) and a volume ΔV of suspen-

sion with initial volume fraction of solids ϕ_{s0} was introduced carefully onto the top of the suspension.

Figs. 1 and 2 show the variation of the discontinuities and the lines of constant concentration in a batch test and in a semibatch test. Three zones can be distinguished: zone a (constant concentration equal to the initial one), zone b (where the straight lines of constant concentration or characteristic lines — dashed lines in Fig. 1 — arise from the bottom of the cylinder at the beginning of the test), and zone c, where the characteristic lines — dashed lines — arise tangentially from the sediment surface at different values of time in the non-compression range. The compression zone or sediment can also be observed. In this latter zone, the divergent lines of constant concentration arise from the bottom of cylinder at different values of times.

By the methods proposed [6,27], a part of the settling flux density versus the volume fraction curve (from ϕ_{s0} to $\phi_{s2,max}$) can be obtained as shown in Fig. 3. Nevertheless, it must be emphasized that the portion of curve that can be obtained by the semi-batch test is greater than that obtained from the single batch test.

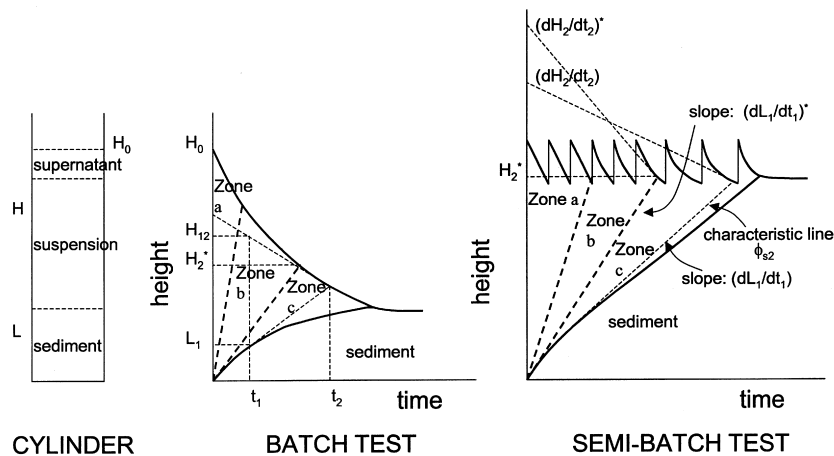


Fig. 2. Batch test and semi-batch test. Symbols used in zones c and for estimation of the critical or gel concentration.

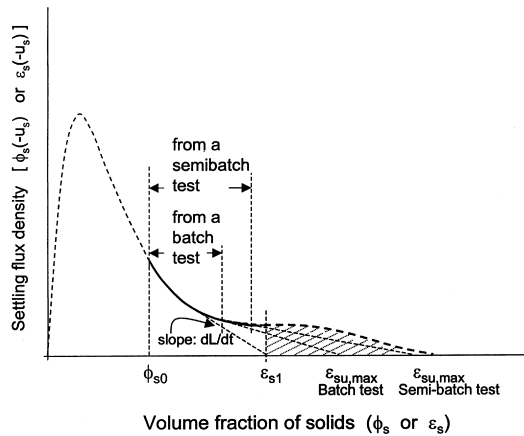


Fig. 3. Settling flux density versus volume fraction of solids.

The different values of the settling flux density, product of the settling rate ($-u_s$) by the solids concentration ϕ_s at the range drawn as a solid line in Fig. 2 can be obtained as follows:

(a) from the straight lines of the supernatant–suspension descending interface observed in the batch test and in the semibatch test, the settling rate value corresponding to the initial solids concentration ϕ_{s0} can be obtained.

(b) for the characteristic lines (of constant solids concentration above the sediment) that arise from the bottom, the values of the settling rates are obtained as dH_2/dt_2 at the interface corresponding to the volume fractions of solids calculated as [22,27]

$$\phi_s = (\phi_{s0}H_0/H_i) \quad \text{for the batch test} \quad (1)$$

$$\phi_s = \phi_{s0} \left(H_0 + \sum_i \Delta H_{0,i} \right) / H_i \quad \times \text{ for the semi-batch test} \quad (2)$$

where H_0 is the initial height of suspension with initial volume fraction ϕ_{s0} , and $\Delta H_{0,i}$ is the increment of suspension height with fresh suspension with solids concentration ϕ_{s0} after withdrawing supernatant from the beginning of the test to the corresponding time.

For each characteristic line corresponding to a volume fraction ϕ_s (Fig. 1), the settling rate is calculated from the slope of the upper discontinuity ($-dH_2/dt_2$), the volume fraction of solids by Eq. (1) and the settling flux density by the product ($-dH_2/dt_2$) ϕ_s .

For the characteristic lines that arise from the sediment (Fig. 2), whose settling rates are also calculated as dH_2/dt_2 , the volume fraction of solids (indicated by ϕ_{s2} in this case and indicated also as ϕ_{s2} in Fig. 2) is obtained by the expression [6,27]:

$$\phi_{s2} = \frac{\phi_{s0}H_0}{H_{12} - L_1} \left[- \int_0^{t_1} \frac{1}{t_2 - t_1} dt \right] \quad \text{for the batch test} \quad (3)$$

$$\phi_{s2} = \frac{\phi_{s0} \left(H_0 + \sum_i \Delta H_{0,i} \right)}{H_i^*} \times \exp \left[- \int_{(dH_2/dt_2)^*}^{(dH_2/dt_2)} \frac{d(-dH_2/dt_2)}{(dH_2/dt_2)^* (dL_1/dt_1) + (-dH_2/dt_2)} \right] \quad \text{for the semi-batch test} \quad (4)$$

For the numerical integration of the previous equations, several tangential characteristics must be considered from the first one tangential to the sediment curve at $t_1=0$ (for Eq. (3)) or from (dH_2/dt_2) equal to $(dH_2/dt_2)^*$ (for Eq. (4)) to the corresponding characteristic with value t_1 for (dH_2/dt_2) . Nevertheless, it must be stated that the theory concerning tangential characteristics that leads to Eqs. (3) and (4) is not yet closed.

Multiplying the value ϕ_{s2} by the settling rate in the upper discontinuity ($-dH_2/dt_2$), the product $(-dH_2/dt_2) \phi_{s2}$ equals the flux density. The maximum value, $\phi_{s2,max}$, that can be calculated corresponds to the characteristic with a slope equal to the sediment slope dL_1/dt_1 just before the critical point.

(c) The limit between the non-compression range of solids concentration and the compression zone corresponds to the situation where the solids structure first shows a compressive yield value and is known as the critical or gel volume fraction of solids ε_{s1} . This value can be calculated as [6,27]:

$$\varepsilon_{s1} = \phi_{s0}H_0/H_2^* \quad \text{for the batch test} \quad (5)$$

$$\varepsilon_{s1} = \left(\phi_{s0} \left(H_0 + \sum_i \Delta H_{0,i} \right) \right) / H_2^* \quad \text{for the semi-batch test} \quad (6)$$

where H_2^* is the intercept height of the upper discontinuity with the characteristic that arises tangentially to the sediment at the beginning of the test and separates zone b from zone c (see Fig. 2).

(d) Continuous thickeners can be designed from the data obtained in a batch test or in a semi-batch test. The sludge withdrawn from the bottom of the continuous thickener, normally has a volume fraction of solids greater than the critical volume fraction ε_{s1} . In a continuous thickener, the variation of the solids concentration vs. depth can be similar to that shown in Fig. 4 [16,28–31]. This figure shows the results of a batch test. Consider a characteristic line that arises tangentially to the sediment at height L and with a volume fraction of solids ϕ_{s2} . A continuous thickener can be designed with the previous relationships. In this continuous thickener, three zones can be distinguished: (a) the sediment on the bottom, with an underflow volume fraction of solids ε_{su} at the bottom and solids concentration ε_{s1} at the top of the sediment; (b) a zone with a volume fraction of solids ϕ_{s2} and (c) an upper zone where the initial suspension is introduced into the thickener. The variation of the volume fraction of solids versus the thickener depth is indicated in Fig. 4. In the upper

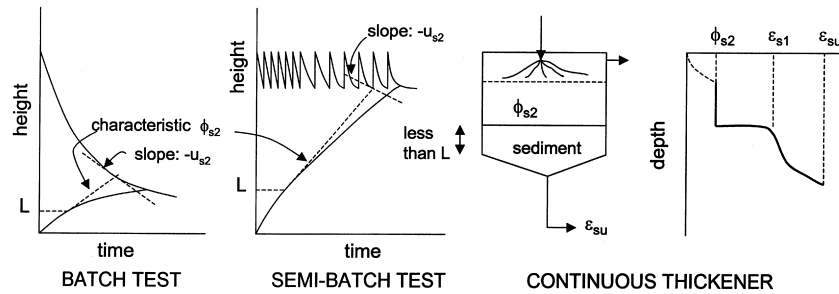


Fig. 4. Batch test, semi-batch test and continuous thickener.

part, the solids concentration is almost zero. In this section, clarified liquid flows out of the thickener. There is a zone where the feed sprays inside the liquid with zones of less concentration than that of the inlet stream.

Above the sediment, there is a layer of constant solids concentration that controls the flux of solids per unit of cross area. Normally, this layer has a solids concentration inside the non-compression range [2,28,29]. In the sediment, there is a gradual variation of solids concentration from ε_{s1} to ε_{su} . At the top of the sediment, there is a great change of solids concentration at a small increment of height (corresponding to a discontinuity). In accordance with that deduced previously [6,25] and considering the material balances, for a characteristic line of a specific volume fraction of solids ϕ_{s2} in Fig. 4, the corresponding parameters of the design of a continuous thickener that has a volume fraction of solids equal to ϕ_{s2} in the zone above the sediment as indicated in Fig. 4, can be obtained as follows:

- Underflow volume fraction of solids ε_{su}

$$\varepsilon_{su} = \phi_{s2} \left(1 + \left((-u_{s2}) / (dL_1/dt_1) \right) \right) \quad (7)$$

(values of ϕ_{s2} , $(-u_{s2}) = -dH_2/dt_2$ and dL_1/dt_1 correspond to the characteristic line of volume fraction ϕ_{s2} arising from the sediment surface).

- Thickener volumetric flux density of solids, θ , related to the unit area or cross area per unit of volumetric flow of solids, A_u .

$$A_u = 1/\theta = 1/(\varepsilon_{su} dL_1/dt_1) \quad (8)$$

- Compression zone height or sludge depth H_u of the continuous thickener. It was deduced that the value H_u is less than the sediment height L_1 just at the point where the drawn characteristic line of volume fraction ϕ_{s2} arises from the top of the sediment [25].

In Fig. 3, for a suspension with an initial volume fraction of solids ϕ_{s0} , any value of underflow volume fraction of solids ε_{su} can be related to a value ϕ_{s2} and can be calculated by the procedure presented previously. The value dL_1/dt_1 is the positive value of the slope of the straight line drawn between the point on the settling flux density–solids concentration curve at ϕ_s (volume fraction of solids above

the compression zone in the gravity thickener) and the underflow volume fraction of solids ε_{su} on the x -axis (this can be easily deduced from a material balance in accordance with the Coe and Clavenger method [8]). Consequently, the greatest value, $\varepsilon_{su,max}$, corresponds to $\phi_{s2,max}$ as observed in Fig. 3.

On considering the previous analysis, it can be deduced that the greatest design value of the underflow volume fraction ε_{su} in the continuous thickener corresponds to the characteristic with greater solids concentration. This characteristic line is that which arises from the sediment surface just before the critical point in the batch test (intercept of the upper discontinuity and the sediment discontinuity, Figs. 1 and 2). The parameters of design that can normally be obtained from a batch test correspond to small sediment heights (e.g. for a batch test similar to that shown in Figs. 1 and 2. If the initial height of the suspension is 1 m, under the conditions corresponding to the characteristic that arises from the sediment surface just before the critical point, the sludge depth in a continuous thickener will then be less than 0.2 m). Any procedure that results in high values of the critical point heights will permit the design parameters of continuous thickeners at great values of underflow solids concentration to be determined. Bearing in mind that the initial solids concentration cannot be changed, one alternative for obtaining high sediment heights consists in carrying out the batch test in very tall cylinders. Another alternative is performing a semi-batch test where the sediment surface must be estimated, as explained in this paper.

This paper focuses the determination of the sediment surface from a semi-batch test, considering the Kynch theorems applied to the hindered settling or non-compression zone above the sediment in a semi-batch test of a flocculated suspension.

2. Fundamentals of the estimation of the sediment surface

Consider Fig. 5, where a characteristic line of a semibatch-test is drawn (solid line). Note that this characteristic line passes by the point just before the fresh suspension added. This means that all the solids of an addition

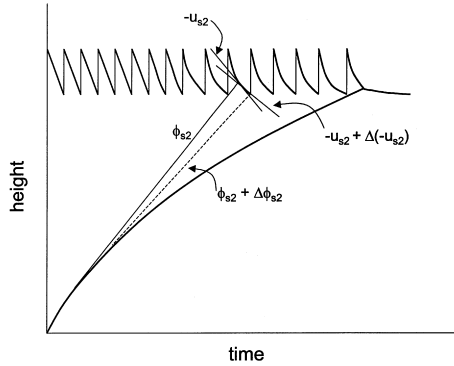


Fig. 5. Characteristic lines in a semi-batch test.

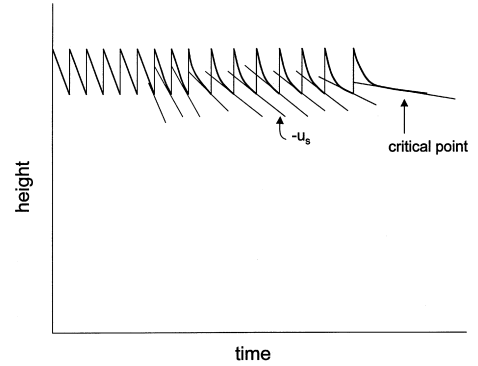


Fig. 6. Determination of settling rates in a semi-batch test.

of suspension at the top of the interface cross the rising characteristic line drawn with constant volume fraction of solids ϕ_s and constant settling rate $(-u_s)$. Consequently from a balance of solids, it is deduced that

$$\phi_s (-u_s) = \phi_{s0} \Delta H_{0,i} / \Delta t \quad (9)$$

where ϕ_{s0} is the volume fraction of solids corresponding to the added fresh suspension, that coincides with the initial solids concentration of the suspension introduced in the cylinder, $\Delta H_{0,i}$ is the increase of the upper interface due to the addition of fresh suspension and Δt is the period of time between two consecutive additions. If the sediment surface height is known, the value $(-u_{s2})$ should be that measured drawing the tangent at the point where the characteristic line intercepts the upper discontinuity. Nevertheless, the variation of $(-u_{s2})$ of the layers at the top of the supernatant–suspension discontinuity inside the same portion of curve between fresh suspension additions must be small when the number of additions is high, because the change of the slope from the characteristic line corresponding to ϕ_{s2} to that corresponding to $\phi_{s2} + \Delta\phi_{s2}$ is small. When the sediment surface height is unknown, as occurs in the opaque suspensions (common case), the settling rate $(-u_{s2})$ can be estimated drawing the tangent at the last portion of the descending discontinuity, as shown in Fig. 5. On the other hand, the characteristic arises with a slope ν that equals

$$\nu = - \frac{d [(-u_s) \phi_s]}{d\phi_s} \quad (10)$$

in accordance with the Kynch theorems [22,5]. These two aspects, the estimation of the value ϕ_{s2} and the use of the relation (10) referring to the rise of the characteristic lines are the fundamentals of the method for estimating the sediment surface height. This is explained in the following paragraphs.

Consider a semi-batch test as that presented in Fig. 6. The settling rate is measured at the last portion of the lines corresponding to the upper discontinuity before the following additions, as indicated in the graph.

With the values of ϕ_s and $(-u_s)$, calculated by Eq. (9), a graph similar to that shown in Fig. 7 can be obtained, where the variation of the settling flux density is plotted vs. the

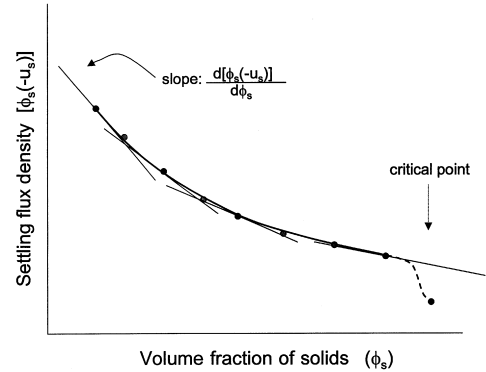


Fig. 7. Estimation of the settling flux density–volume fraction of solids variation.

volume fraction of solids. Drawing tangents to the curve at the points considered, arising rates of the characteristic lines are obtained in accordance with Eq. (10). This means that for each point considered in Fig. 6 before a new addition of fresh suspension, the values ν of the slopes of the characteristics can be estimated. Drawing lines with these slopes from the corresponding points, as indicated in Fig. 8, the sediment curve must be tangent to all these lines, and consequently an estimation of the sediment surface is obtained. With the estimated sediment surface, the rigorous procedure for designing continuous gravity thickeners can be used.

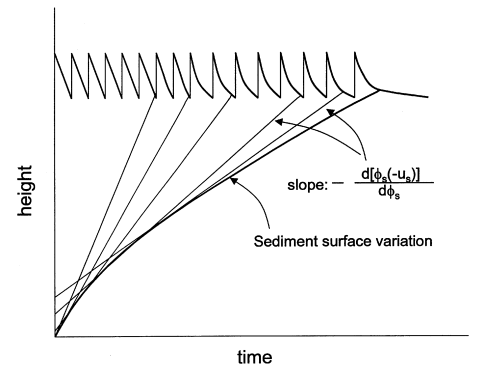


Fig. 8. Drawing of the characteristic lines and the estimated sediment surface in a semi-batch test.

The critical point, where the sediment curve meets the upper interface, can also be deduced from Fig. 6, because normally a noticeable increase of Δt between additions takes place.

3. Corroboration of the method proposed with data obtained by simulation

A simulation program of the batch testing was initially developed [13], where the variations of the upper discontinuity height, sediment height, characteristic lines and lines of constant solids concentration inside the sediment versus time were considered. Afterwards, the simulation program was developed for considering the simulation of a gravity thickener and dimensionless variables were taken into account [20]. The most important relationships considered in this last paper with the general case analyzed were the following:

- In the hindered settling zone: relationship between the settling rate ($-u_s$) and the volume fraction of solids ϕ_s

$$(-u_s) = (-u_{s0}) (1 - j\phi_s)^{4.65} \quad \text{for } 0 < j\phi_s < 0.64 \quad (11)$$

$$j = j_0 - (j_0/2.56)\phi_s$$

in accordance with the Richardson and Zaki [32] relationship and assuming a variation for the parameter j with the volume fraction of solids ϕ_s .

- At the critical or gel concentration ε_{s1} , the value of $j\varepsilon_{s1}$ equals 0.64, and considering that the value of j at ε_{s1} equals $j_0/2$, the product $j_0\varepsilon_{s1}$ is equal to 1.28.
- In the compression zone: relationship between the effective pressure p_s and the volume fraction of solids ε_s , in accordance with the relation of Tiller and Khatib [33]

$$\varepsilon_s = \varepsilon_{s\infty} - (\varepsilon_{s\infty} - \varepsilon_{s1}) e^{-p_s/p_B} \quad (12)$$

where $\varepsilon_{s\infty}$ is assumed to be $2\varepsilon_{s1}$.

relationship between the terminal settling rate ($-u_{st}$) (in absence of compressive stress) or the permeability k :

$$(-u_{st}) = (\Delta\rho g \varepsilon_s k / \mu)$$

$$= \left[6.3095 \times 10^{-5} (-u_{s0}) / (\varepsilon_s j_0) \right]$$

$$\times \{ \text{ATN} [-10 (j_0 \varepsilon_s - 1.92)] \} + 90 \quad (13)$$

The previous equation corresponds to a general variation case.

Introducing the dimensionless variables:

$$\phi_s^+ = j_s \phi_s \quad 0 < \phi_s^+ < 1.28 = \varepsilon_{s1}^+ \quad (14)$$

$$\varepsilon_s^+ = j_0 \varepsilon_s \quad 1.28 = \varepsilon_{s1}^+ < \varepsilon_s^+ < 2.56 = \varepsilon_{s\infty}^+ \quad (15)$$

$$t^+ = (\Delta\rho g (-u_{s0}) / p_B) t \quad (16)$$

$$x^+ = (\Delta\rho g / (j_0 p_B)) x \quad (17)$$

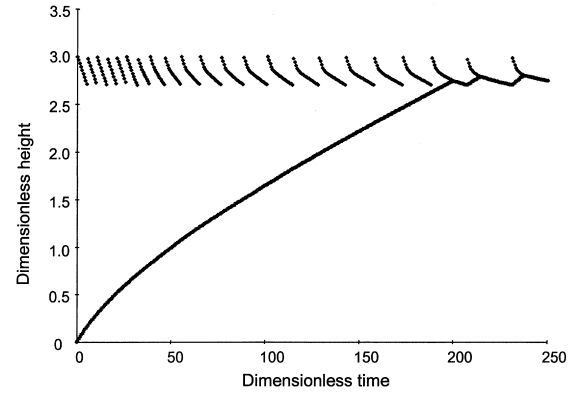


Fig. 9. Simulated data of the supernatant–suspension height and sediment height versus time.

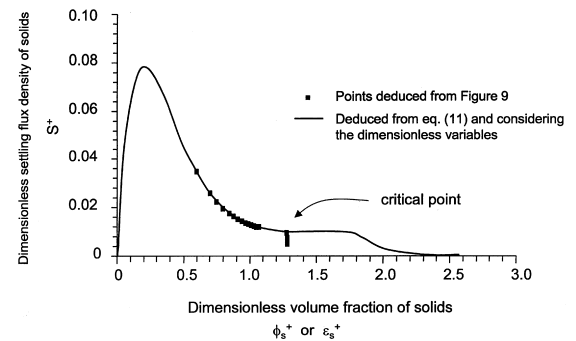


Fig. 10. Dimensionless flux density versus volume fraction of solids.

the simulation of the batch was carried out as presented elsewhere [20,27].

Fig. 9 shows the simulated data of the variation of the upper discontinuity and sediment height versus time.

Considering only the simulated data of the upper discontinuity, the procedure previously explained was applied. Fig. 10 shows the variations of the settling flux density S^+ ($=(-u_s^+)\phi_s^+$) obtained by the procedure previously explained and that deduced from the equations used (from Eq. (11)) considering the dimensionless variables, observing an exact coincidence.

Fig. 11 shows the drawing of the characteristic lines and the estimated sediment surface, that coincides with the simulated data of sediment surface.

Consequently, from the simulated data, in the absence of experimental errors and deviation of the model assumed, it can be deduced that the model developed is rigorous and exact.

4. Corroboration of the method proposed with experimental data

In a previous paper [27], some experimental data of semi-batch test with calcium carbonate suspensions were presented. With these suspensions, the sediment surface

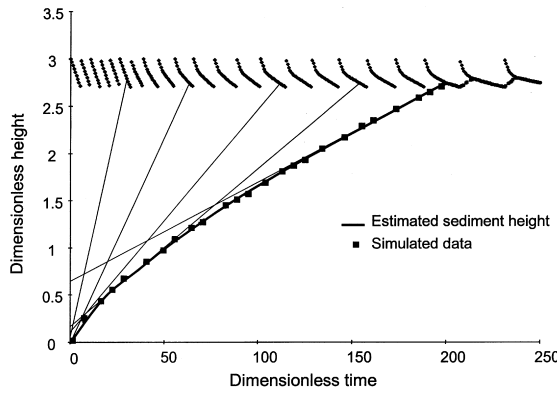


Fig. 11. Drawing of characteristic lines and the estimated sediment height from the simulated data.

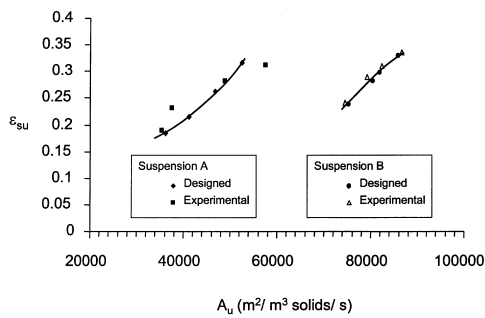


Fig. 12. Experimental and designed underflow volume fraction versus unit area for two calcium carbonate suspensions: suspension A and suspension B.

was visible, and it was also tested that the procedure commented previously for the design of gravity thickeners considering the data of the sediment surface was correct. Figs. 12 and 13 show the design and operation variables, underflow solids concentration, sediment height and unit area, obtained with two suspensions of calcium carbonate, with different hydrodynamic behavior. More details about the operation procedure can be found elsewhere [27].

The procedure for estimating the sediment surface was applied to these experimental data and compared with the calculated ones. Figs. 14 and 15 show the experimental data

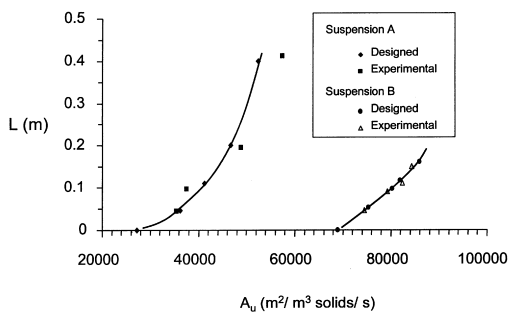


Fig. 13. Experimental and designed sediment height versus unit area for two calcium carbonate suspensions: suspension A and suspension B.

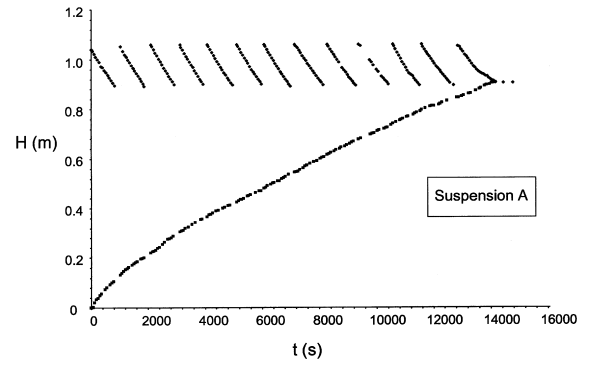


Fig. 14. Supernatant–suspension height and sediment height versus time for suspension A of calcium carbonate.

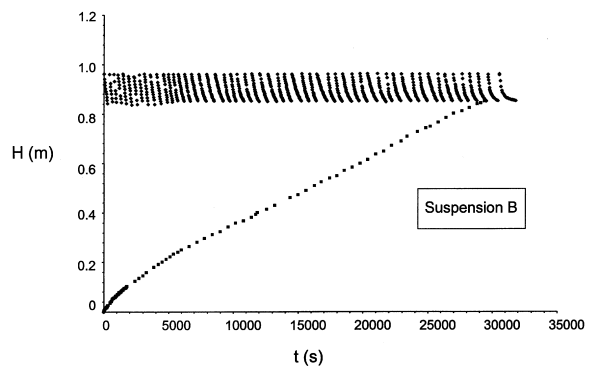


Fig. 15. Supernatant–suspension height and sediment height versus time for suspension B of calcium carbonate.

of the variation of the upper discontinuity and the sediment surface. Considering only the experimental data of the upper discontinuity and following the procedure previously presented, the variation of the settling flux density versus volume fraction of solids is deduced (shown in Fig. 16) and used for calculating the slope of the characteristics drawn in Figs. 17 and 18, showing that the estimated sediment surface coincides with the experimental value, and corroborates the procedure proposed.

Similar results, corroborating the procedure for estimating the sediment surface in a semi-batch test of sedimenta-

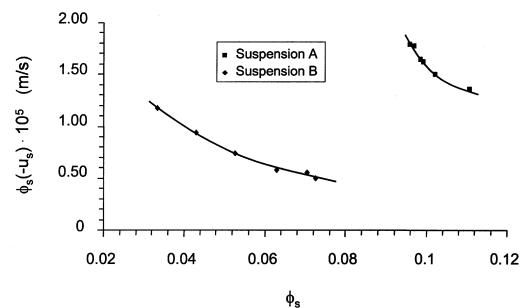


Fig. 16. Flux density versus volume fraction of solids for both calcium carbonate suspensions.

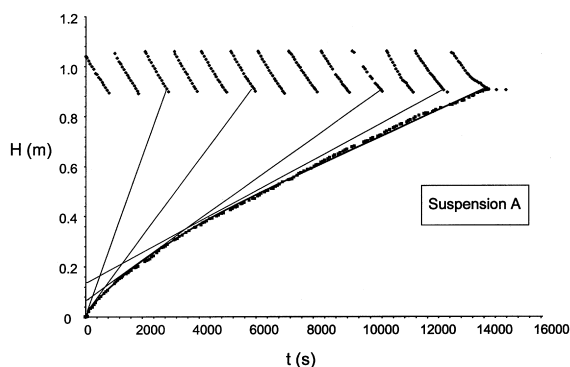


Fig. 17. Drawing of characteristic lines and the estimated sediment height for suspension A of calcium carbonate.

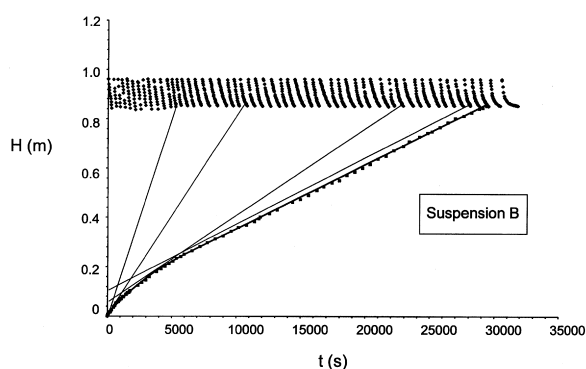


Fig. 18. Drawing of characteristic lines and the estimated sediment height for suspension B of calcium carbonate.

tion, have been obtained with other suspensions of calcium carbonate, and metal hydroxides.

5. Conclusions

From a semi-batch test, where periodically the supernatant is withdrawn and a volume of suspension is added, the sediment surface can be obtained and consequently the design values of the unit area and the sediment height of continuous thickeners can be deduced, thus extending the intervals of the parameters that can be deduced from batch testing.

The method proposed for obtaining the sediment surface was successfully tested with simulated data (where the upper discontinuity height and the sediment height variations were known) and with experimental values of calcium carbonate suspensions where the sediment surface was also visible; consequently the sediment height variation versus time could be compared with that estimated by application of the method proposed.

References

- [1] W.P. Talmage, E.B. Fitch, *Ind. Eng. Chem.* 47 (1955) 38.
- [2] B. Fitch, *AIChE J.* 25 (1979) 913.
- [3] M. Merta, J. Ziolo, *Chem. Eng. Sci.* 40 (1985) 1301.
- [4] M. Merta, J. Ziolo, *Chem. Eng. Sci.* 41 (1986) 1918.
- [5] B. Fitch, *AIChE J.* 29 (1983) 940.
- [6] R. Font, *AIChE J.* 34 (1988) 229.
- [7] K. Yong, H. Xiaomin, D. Changlie, et al. *Trans. Nonferrous Met. Soc. China* 6 (1996) 29.
- [8] H.S. Coe, G.H. Clavenger, *Trans. Am. Inst. Mining Engrs.* 55 (1916) 356.
- [9] M. Donald, R. Riddell, J.S. Lee, et al. *J. Water Pollut. Control Fed.* 55 (1983) 360.
- [10] D.C. Dixon, *J. Water Pollut. Control Fed.* 57 (1985) 46.
- [11] A.G. Waters, K.P. Galvin, *Filtr. Sep.* 28 (1991) 110.
- [12] A.G. Foust, L.A. Wenzel, C.W. Clump, et al., *Principles of Unit Operations*, Wiley, New York, 1960 (Chapter 22).
- [13] R. Font, *Chem. Eng. Sci.* 46 (1991) 2473.
- [14] B. Fitch, *Ind. Eng. Chem.* 58 (1966) 18.
- [15] K.A. Landman, L.R. White, R. Buscall, *AIChE J.* 34 (1988) 239.
- [16] F.M. Tiller, W. Chen, *Chem. Eng. Sci.* 43 (1988) 1695.
- [17] D.C. Dixon, *AIChE J.* 26 (1980) 471.
- [18] D.C. Dixon, *Chem. Eng. Sci.* 36 (1981) 499.
- [19] B. Fitch, *AIChE J.* 36 (1990) 1545.
- [20] R. Font, F. Ruiz, *Chem. Eng. Sci.* 48 (1993) 2039.
- [21] R. Bürger, F. Concha, *Int. J. Multiphase Flow* 24 (1998) 1005.
- [22] G.J. Kynch, *Trans. Faraday Soc.* 48 (1952) 166.
- [23] B. Fitch, *AIChE J.* 39 (1993) 27.
- [24] F.M. Tiller, *AIChE J.* 27 (1981) 823.
- [25] R. Font, *AIChE J.* 36 (1990) 3.
- [26] R.G. Holdich, G. Butt, *Sep. Sci. Technol.* 32 (1997) 2149.
- [27] R. Font, M.L. Laveda, *Chem. Eng. Sci.* 51 (1996) 5007.
- [28] E.W. Comings, C.E. Pruess, C. Debord, *Ind. Eng. Chem.* 46 (1954) 1164.
- [29] K.J. Scott, *Ind. Eng. Chem. Fundam.* 9 (1970) 422.
- [30] A.R. Tarrer, H.C. Lim, L.B. Koppel, et al. *Ind. Eng. Chem. Process Des. Devel.* 13 (1974) 341.
- [31] J.S. Turner, D. Glasser, *Ind. Eng. Chem. Fundam.* 15 (1976) 23.
- [32] J.F. Richardson, W.N. Zaki, *Trans. Instn. Chem. Engrs.* 32 (1954) 35.
- [33] F.M. Tiller, Z. Khatib, *J. Colloid Interface Sci.* 100 (1984) 55.